CHAOS 28, 075512 (2018)

Nonlinear convection of binary liquids in a porous medium

Y. Rameshwar,[1] V. Anuradha,[2] G. Srinivas,[1] L. M. Pérez,[3] D. Laroze,[3,4,a)] and H. Pleiner[5]
[1)] *Department of Mathematics, University College of Engineering, Osmania University, Hyderabad, 500007, India*
[2)] *Department of Mathematics, Government Degree College for Women, Begumpet, Hyderabad, 500007, India*
[3)] *School of Physical Sciences and Nanotechnology, Yachay Tech University, 00119 - Urcuquí, Ecuador*
[4)] *Instituto de Alta Investigación, CEDENNA, Universidad de Tarapacá, Casilla 7D, Arica, Chile*
[5)] *Max Planck Institute for Polymer Research, D 55021 Mainz, Germany*

(Received 02 March 2018; accepted 09 March 2018; published online 20 July 2018)

Thermal convection of binary mixtures in a porous medium is studied with stress-free boundary conditions. The linear stability analysis is studied by using the normal mode method. The effects of the material parameters have been studied at the onset of convection. Using a multiple scale analysis near the onset of the stationary convection a cubic-quintic amplitude equation is derived. The influence of the Lewis number and the separation ratio on the supercritical-subcritical transition is discussed. Stationary front solutions and localized states are analyzed at the Maxwell point. Near the threshold of the oscillatory convection, a set of two coupled complex cubic-quintic Ginzburg-Landau type amplitude equations is derived, and implicit analytical expressions for the coefficients are given. *Published by AIP Publishing.* https://doi.org/10.1063/1.5027468

Thermal convection of binary liquids in a porous medium is considered, since it exhibits both, stationary and oscillatory instabilities that allow for transitions from a supercritical, forward bifurcation to a subcritical, backward one. The latter regime features the coexistence and competition between different states and is described by generalized Ginzburg-Landau type equations. We derive those equations for rather general cases and discuss analytically, for the stationary instability, front propagation, and localized states.

I. INTRODUCTION

Recent developments in both, theoretical and experimental fluid dynamics, have stimulated widespread interest in nonlinear physics problems. The understanding of convection has fundamental importance in everyday life, geophysics as well as astrophysics.[1] For instance, convection in binary liquid mixtures in porous media is pertinent for transport processes in geothermal reservoirs[2] and industrial developments.[3,4]

Instabilities in porous media have extensively been studied theoretically in the literature.[5–15] The linear stability analysis was performed by Brand and Steinberg for binary fluids.[6] The standard, cubic amplitude equations for stationary and oscillatory instability were derived for different situations.[7–10] In the stationary case, a real cubic-quintic amplitude equation was analyzed.[11] Numerical works have also been presented.[12–15] In particular, a Galerkin method for a 3-dimensional situation was recently employed.[15]

In this article, we report theoretical and numerical results concerning thermal convection of binary liquids in a porous medium. The latter is characterized by a porosity number, while the binary fluid is described by the Lewis number (due to mass diffusion) and the separation ratio, which we take as negative (positive Soret coefficient). The system is driven by heating from below described by a positive Rayleigh number and we assume idealized boundary conditions (Sec. II). For finite porosity, linear stability allows for a stationary and an oscillatory instability, and we show the ratio of the appropriate thresholds (critical Rayleigh numbers) as a function of the material parameters (Sec. III).

The aim of this work is to characterize the subcritical regime of binary fluids in porous media for idealized boundary conditions. Using the standard weakly nonlinear description based on multiple scale analysis, we derive partial differential equations for the slowly varying amplitudes, i.e., the envelopes of the convective flow (roll patterns). Interested in the subcritical regime, a (real) cubic-quintic Ginzburg-Landau type equation is obtained in the stationary case (Sec. IV A), while for the oscillatory one a coupled set of two complex cubic-quintic Ginzburg-Landau type equations is found (Sec. IV C). Within the subcritical regime of the stationary instability, localized states are found analytically, which are stable at the Maxwell point, but decay away from it (Sec. IV B). For the oscillatory convection, we give analytical expressions for the complex coefficients of the amplitude equations (Appendix).

II. THERMAL CONVECTION MODEL

In a porous medium we consider a planar layer of an incompressible binary mixture of thickness d, with very large horizontal extensions in the x and y direction and subject to a vertical gravitational field $\mathbf{g}$ as well as a ver-

[a)] Corresponding author: dlarozen@uta.cl

tical temperature gradient. We choose the z-axis such that $\mathbf{g} = -g_E \hat{e}_z$ and the boundaries of the layer to be at $z = 0$ and $z = d$. A static temperature difference across the layer is imposed, $T(z=0) = T_0 + \Delta T$ and $T(z=d) = T_0$. In the Boussinesq approximation we consider the fluid as incompressible except when dealing with the buoyancy force due to the temperature gradient. Within this approximation the equations that describe perturbations of the heat conducting state are given[6] in dimensionless form as

$$(1+\chi\partial_t)\nabla^2 w - \nabla_\perp^2\theta - \psi\nabla_\perp^2 C = 0, \tag{1}$$

$$(\partial_t + \mathbf{v}\cdot\nabla - \nabla^2)\theta - Ra\, w = 0, \tag{2}$$

$$(\partial_t + \mathbf{v}\cdot\nabla - L\nabla^2)C + L\nabla^2\theta - Ra\, w = 0, \tag{3}$$

where $\mathbf{v} = (u,v,w)^T$ is the velocity field, θ the temperature field, C the concentration field of the denser component, and $\nabla_\perp^2 f = \partial_x^2 f + \partial_y^2 f$. In Eqs. (1)-(3), several groups of dimensionless numbers have been introduced: **(*a*)** (fluids) the Rayleigh number, $Ra = \alpha_T g_E K d^3/\kappa\nu$, accounting for buoyancy effects, and the porosity number, $\chi = (K\kappa)/(\mu\nu d^2)$ characterizing the medium, and **(*b*)** (binary mixture) the separation ratio, $\psi = -\alpha_C S_T/(\alpha_T T_0)$ and the Lewis Number, $L = D/\kappa$, relating diffusion with thermal diffusivity. Here κ is the thermal diffusivity, ν is the viscosity, α_T is the thermal expansion coefficients, α_C is the mass expansion coefficient, S_T is the thermodiffusion ratio, D is the diffusion constant, K is permeability, and μ is the porosity of a porous medium. We remark that, due to the Soret effect, binary fluids subject to a temperature gradient experience a stratification of the solute concentration, hence the separation ratio is an important control parameters.

The aforementioned equations can be written in a compact operator form

$$\mathscr{L}\mathbf{u} + \mathscr{N}(\mathbf{u},\mathbf{u}) = 0 \tag{4}$$

with $\mathbf{u} = (\mathbf{v},\theta,C)^T$, and the corresponding linear, $\mathscr{L}$, and nonlinear operator, $\mathscr{N}$. On both boundaries, $z = (0,1)$ idealized, stress free boundary conditions are imposed.[1] At the boundaries there are no temperature or concentration fluctuations $w = \theta = C = 0$. Periodic boundary conditions are used in the horizontal directions. Thus, the z-dependence of the fields $\mathbf{u}$ is entirely given by appropriate trigonometric functions.

This system has different types of instabilities,[6–9,11] e.g., stationary and oscillatory, with the possibility of a co-dimension two bifurcation. Which type of bifurcation occurs, depends on the control parameters, in particular on the separation ratio ψ and the Lewis number L. We first briefly review the linear stability analysis.

III. LINEAR STABILITY ANALYSIS

We study the linear stability using a normal mode expansion. For the linear case the set of equations (1) - (3)

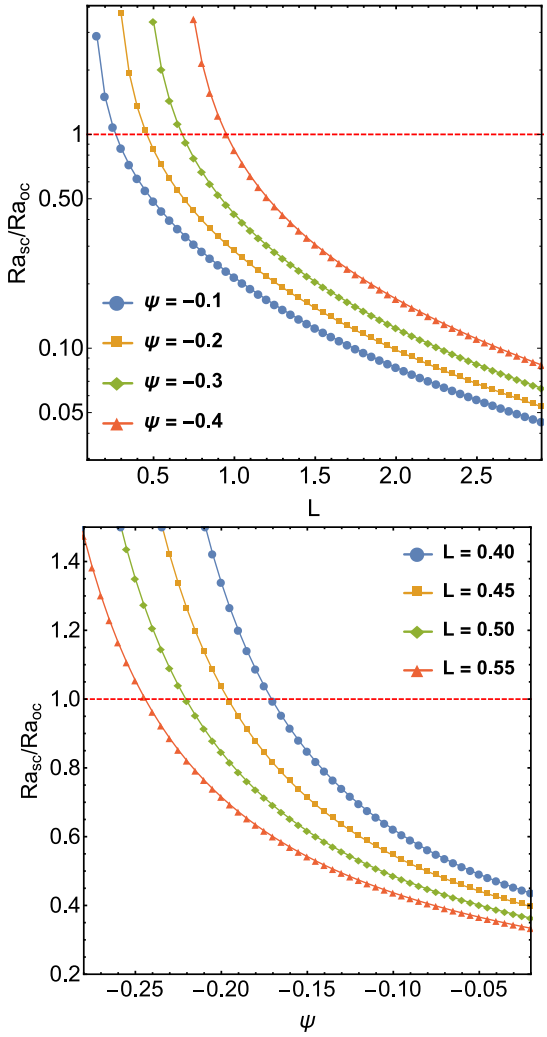

FIG. 1. Ratio of the critical Rayleigh numbers R_{sc}/R_{oc} as a function of the Lewis number L (top) and of the separation ratio ψ (bottom) for $\chi = 1$.

can be reduced to $\mathscr{L}_w w = 0$ where the linear operator $\mathscr{L}$ can be written as

$$\mathscr{L}_w = \left(\frac{\partial}{\partial t} - \nabla^2\right)\left(\frac{\partial}{\partial t} - L\nabla^2\right)\left(1 + \chi\frac{\partial}{\partial t}\right)\nabla^2 + Ra\left[\psi L\nabla^2 - \psi\left(\frac{\partial}{\partial t} - \nabla^2\right) - \left(\frac{\partial}{\partial t} - L\nabla^2\right)\right]\nabla_z^2 \tag{5}$$

According to the boundary conditions one tries solutions of the form $w = \exp(iqx + pt)\sin(\pi z)$, where q is the transverse wavevector and $p = \sigma + i\omega$ is the complex eigenvalue with σ the growth rate of perturbation and ω its frequency. This ansatz produces a solvability condition for Ra.

A. Stationary convection

For for onset of the stationary convection, $p = 0$, and the Rayleigh number is given by Ref. 6

$$Ra_s = \frac{\delta^4}{q^2\left(1+\psi+\frac{\psi}{L}\right)}, \tag{6}$$

where $\delta^2 = \pi^2 + q^2$. The minimum of the marginal curve $Ra_s(q)$, given by $\partial_q Ra_s = 0$, determines the critical wavenumber q_{sc} and, subsequently, the critical Rayleigh number, $Ra_{sc} = Ra_s(q_{sc})$, of the most unstable perturbation. In this case one gets $Ra_{sc} = (4\pi^2)/(1+\psi+\psi/L)$ and $q_{sc} = \pi$.

B. Oscillatory convection

The oscillatory convection occurs when $p = i\omega$. In this case, the Rayleigh number and frequency are given by

$$Ra_o = \frac{\delta^4(1+L)\left[\delta^4\chi^2 L + \delta^2\chi(1+L)+1\right]}{q^2(1+\psi+\chi\delta^2)} \tag{7}$$

and

$$\omega^2 = -\frac{\delta^4\left[\left(1+\chi\delta^2\right)\left[L^2(1+\psi)+\psi L\right]+\psi\right]}{1+\chi\delta^2+\psi}. \tag{8}$$

To calculate the oscillatory thresholds, again one first determines the critical wave number q_{oc} (via $\partial_q Ra_o = 0$) leading to the critical Rayleigh number $Ra_{oc} = Ra_o(q_{oc})$ and critical frequency $\omega_{oc} = \omega(q_{oc})$. Generally, this has to be done numerically, but in the case $\chi \ll 1$, relevant for many experimental systems, analytical results are possible. In particular, the critical values are

$$q_{oc} = \pi \tag{9}$$

$$R_{oc} = 4\pi^2(1+L)/(1+\psi) \tag{10}$$

$$\omega_{oc}^2 = -4\pi^4(L^2+\psi[L^2+L+1])/(1+\psi) \tag{11}$$

in that approximation. These results are in agreement with Ref. 7–9. Finally, we remark that the system admits a co-dimension two bifurcation. In fact, in the limit $\chi \ll 1$, the Takens-Bogdanov bifurcation point ($\omega_c^2 = 0$) occurs at $\psi = -L^2/(1+L+L^2)$. It should be mentioned, however, that for $\chi = 0$ the oscillatory instability is always unstable with respect to the stationary one. Only by heating from above a linear oscillatory instability is possible in this limit.[6]

Figure 1 shows the ratio between the critical Rayleigh numbers of the stationary and oscillatory convection, Ra_{sc}/Ra_{oc}, as a function of the Lewis number L (top) and the separation ratio ψ (bottom). These are numerical results for the case $\chi = 1$. Obviously, the oscillatory instability is favoured ($Ra_{sc}/Ra_{oc} > 1$) for smaller L (at fixed negative ψ) and for smaller (more negative) ψ (at fixed L), and in particular, if both are small.

IV. WEAKLY NONLINEAR ANALYSIS

A nonlinear analysis is needed to determine the type of convective motion, which is expected to develop beyond the linear instability threshold. The study of the evolution of the convective pattern can be done by means of a multiple scale analysis.[16–18] Close to the thresholds it is assumed that the amplitude of the basic solution changes only slowly in time and space on the scales $T = \varepsilon^2 t$ and $X = \varepsilon x$, respectively. The small expansion parameter is $\varepsilon^2 = (Ra - Ra_c)/Ra_c$, where Ra_c is the critical value for the stationary or the oscillatory instability. These two cases will be analyzed below.

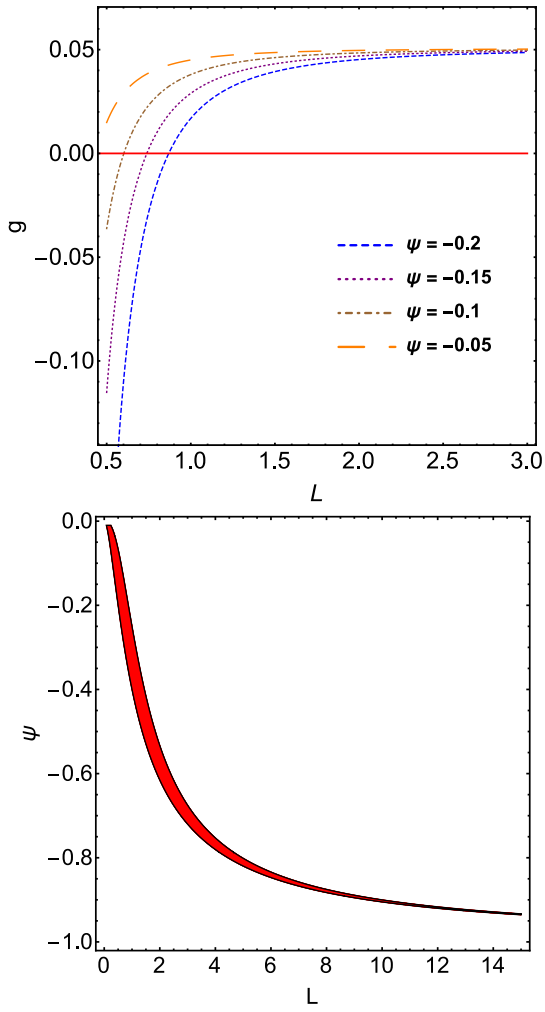

FIG. 2. Top: The cubic coefficient g as a function of L for different values of ψ. Bottom: Existence range for subcritical behavior ($g < 0$ and $\tau_0 > 0$) in the L - ψ plane for $\chi = 1$.

A. Onset of stationary convection

To solve Eq. (4) iteratively, one expands the functions, $\mathbf{u} \to \varepsilon\left(\mathbf{u}_0 + \varepsilon^{1/2}\mathbf{u}_1 + \varepsilon\mathbf{u}_2 + \ldots\right)$ and the operators $\mathscr{L} \to \mathscr{L}_0 + \varepsilon^{1/2}\mathscr{L}_1 + \varepsilon\mathscr{L}_2 + \varepsilon^{3/2}\mathscr{L}_3 + \ldots$ and $\mathscr{N} \to \varepsilon^{3/2}\mathscr{N}_0 + \varepsilon^2\mathscr{N}_1 + \varepsilon^{5/2}\mathscr{N}_2 + \ldots$, using $\partial_x \to \partial_x + \varepsilon\partial_X$ and $\partial_t \to \varepsilon^2\partial_T$. In $O(\varepsilon)$ the linear problem is obtained. The nonlinearities in Eq. (4) generate corrections in higher orders. The solvability criterion for the last correction yields an equations for $A(X,T)$ of the imposed disturbances[19]. This is a Ginzburg-Landau (GL) type equation.

In particular, one obtains a hierarchy of equations: $\mathscr{L}_0\mathbf{u}_0 = 0$, $\mathscr{L}_0\mathbf{u}_1 = \mathscr{N}_0 - \mathscr{L}_1\mathbf{u}_0$, $\mathscr{L}_0\mathbf{u}_2 = \mathscr{N}_1 - \mathscr{L}_1\mathbf{u}_1 - \mathscr{L}_2\mathbf{u}_0$, $\mathscr{L}_0\mathbf{u}_3 = \mathscr{N}_2 - \mathscr{L}_1\mathbf{u}_2 - \mathscr{L}_2\mathbf{u}_1 - \mathscr{L}_3\mathbf{u}_0$ and $\mathscr{L}_0\mathbf{u}_4 = \mathscr{N}_3 - \mathscr{L}_1\mathbf{u}_3 - \mathscr{L}_2\mathbf{u}_2 - \mathscr{L}_3\mathbf{u}_1 - \mathscr{L}_4\mathbf{u}_0$. These equations are inhomogeneous differential equations and at each order one has to fulfill the solvability condition $\langle \mathbf{u}_0^\dagger \mid r.h.s. \rangle = \mathbf{0}$, where $\mathbf{u}_0^\dagger$ is the solution of the linear adjoint problem $\left(\mathscr{L}^+\mathbf{u}^\dagger = 0\right)$. Here, *r.h.s* means the corresponding right hand side in the appropriate order and $< \mid >$ denotes the inner product, which is defined as a suitable volume integration. The solvability condition at $O\left(\varepsilon^{7/2}\right)$ leads to an equation for the amplitude A that is written as

$$\tau_o \frac{\partial A}{\partial T} = \varepsilon^2 A - g|A|^2 A + f|A|^4 A + \xi_o^2 \frac{\partial^2 A}{\partial X^2}. \qquad (12)$$

Equation (12) is the cubic-quintic GL equation with real coefficients describing the variation on the slow time and large spatial scales of the convective pattern. The coefficients τ_0 and ξ_0^2 are the growth rate amplitude and the curvature of the marginal stability curve, respectively. They can be calculated straightforwardly from the linear stability analysis.[19] The material properties g and f are known as the nonlinear coefficients.

When $g > 0$ we get a forward, supercritical bifurcation, while for $g < 0$ the bifurcation is backward and subcritical. The transition point between the sub- and the supercritical bifurcation at $g = 0$ is a tricritical bifurcation point. For the supercritical case, the calculation of the quintic term is not needed, while to analyze the subcritical one the knowledge of the quintic coefficient, f, is necessary. These coefficients are obtained using the standard procedure[19,20] sketched above up to $O\left(\varepsilon^{7/2}\right)$. For idealized boundary conditions, after straightforward calculations, the explicit expressions of these coefficients up to the cubic term can be written as

$$\tau_o = \frac{1}{2\pi^2}\left[\chi + \frac{L^2 + \psi(L^2 + L + 1)}{L(L + \psi L + \psi)}\right], \qquad (13)$$

$$\xi_o^2 = \frac{3}{\pi^2}, \qquad (14)$$

$$g = \frac{1}{2\pi^2}\left[\frac{L^3 + \psi(L^3 + L^2 + L + 1)}{L^2(L + \psi L + \psi)}\right]. \qquad (15)$$

If $\chi \ll 1$ these coefficients are in agreement with the coefficients obtained in Ref. 11, except for a scale factor in g. The analysis of secondary instabilities of the cubic GL equations can be found in Refs. 18,21.

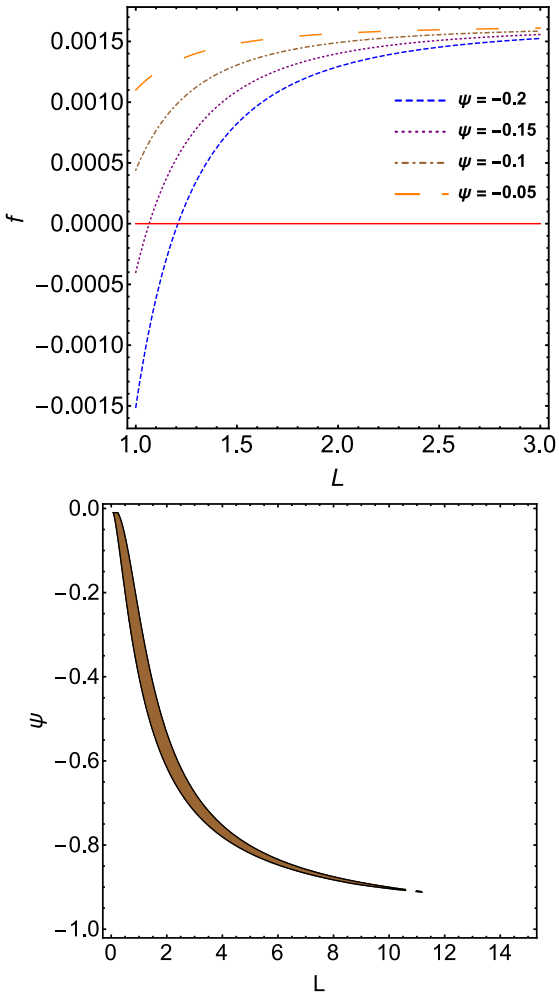

FIG. 3. Top: The quintic coefficient f as a function of L for different values of ψ. Bottom: Existence range for the cubic-quintic amplitude equation ($g < 0$, $f < 0$ and $\tau_0 > 0$) in the L – ψ plane for $\chi = 1$.

The upper part of Fig. 2 shows the coefficient g as a function of the Lewis number L for different values of the separation ratio ψ. It can change sign and is negative for lower values of L and higher (less negative) values of ψ. This also becomes apparent in the lower part of Fig. 2, where the red area shows the range of negative g values in the $L - \psi$ plane. This is the region where the quintic term of the amplitude equation has to be taken into account. The tricritical bifurcation line, where $g = 0$, is given by $\psi = -L^3/(L^3 + L^2 + L + 1)$. For $\psi = -L/(L+1)$ both, g and τ_0 diverge.

To explore the subcritical bifurcation we calculate the

quintic coefficient, which is given by

$$
\begin{aligned}
f = & \frac{1}{8\pi^4\left(1+\psi+\frac{\psi}{L}\right)^2}\left\{\frac{1}{18}\left(1+\psi+\frac{\psi}{L}+\frac{\psi}{L^2}+\frac{\psi}{L^3}\right)^2\right. \\
& \left.+\left(\psi+\frac{\psi}{L}+1\right)\left(1+\psi+\left[\frac{\psi}{L}+\frac{\psi}{L^2}\right]\left[1+\frac{1}{L}+\frac{1}{L^2}+\frac{1}{L^3}\right]\right)\right\} \\
& +\frac{(1+\psi)}{480\pi^4\left(1+\psi+\frac{\psi}{L}\right)^2}\left(1+\psi+\frac{\psi}{L^2}+\frac{\psi}{L^3}\right) \\
& +\frac{\psi}{1920\pi^4\left(1+\psi+\frac{\psi}{L}\right)^2}\left(2+\frac{1}{L}\right)\left(\frac{1}{L}+\frac{\psi}{L}+\frac{\psi}{L^2}+\frac{\psi}{L^3}+\frac{\psi}{L^4}\right) \\
& +\frac{1}{80\pi^4\left(1+\psi+\frac{\psi}{L}\right)}\left(1+\psi+\frac{\psi}{L^2}+\frac{2\psi}{L}\right). \qquad (16)
\end{aligned}
$$

We remark that this result is somewhat different from that obtained in Ref. 11. However, for most of the values of L the different expressions show similar behavior, and for large values of L they converge.

The upper part of Fig. 3 shows the coefficient f as a function of the Lewis number L for different values of separation ratio ψ. One observes that f increases monotonically for increasing L reaching a constant value (for any negative ψ). The quintic coefficient f can only be negative below a certain value of L that increases with decreasing (more negative) ψ values. The condition $f<0$ is necessary for the quintic amplitude equation to be reasonable. The lower part of Fig. 3 shows the $L-\psi$ range, where this is the case. Compared to Fig. 2 the existence range is (slightly) smaller due to the additional condition $f<0$, in particular for $L \gtrsim 11$.

Finally, we remark that homogeneous solutions of this type of equations have been studied in Ref. 11, and the Eckhaus instability of this system in Ref. 21. In the next section we study further stationary solutions in the subcritical regime.

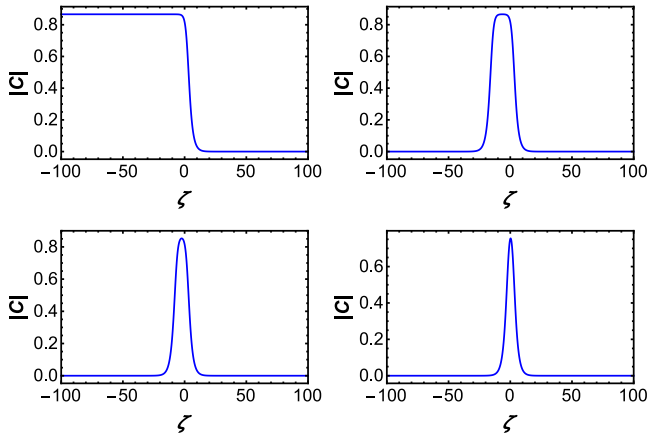

FIG. 4. Stationary front solution and localized states of Eq. (17) at $\mu=\mu_M$ for different values of β: $\beta=1.0$ (top-left), $\beta=0.9999$ (top-right), $\beta=0.999$ (bottom-left), and $\beta=0.9$ (bottom-right). In all cases $\zeta_0=0$.

B. Stationary front solutions and localized states

Since we are interested in the subcritical regime, we rewrite Eq. (12) in the generic form. Using the scaling $C=|g|^{1/2}A$, $\tau=T/\tau_o$ and $\zeta=X/\xi_o$, the amplitude Eq. (12) is reduced to

$$
\frac{\partial C}{\partial \tau}=\mu C+C|C|^2-\beta C|C|^4+\frac{\partial^2 C}{\partial \zeta^2}, \qquad (17)
$$

where $\mu=\sqrt{\varepsilon}$ and $\beta=|f|/\sqrt{|g|}$ such that $\beta>0$. Equation (17) has five stationary homogeneous solutions with the moduli $|C|=0$ and $|C|^2_{\pm}=\left(1\pm\sqrt{1+4\mu\beta}\right)/2\beta$. The former describes the conductive state and the latter are the envelopes of convective states. The trivial solution $|C|=0$ is stable (unstable) for all negative (positive) values of μ. The solution $|C|^2_-$ only exists for $-1/4\beta<\mu<0$, but is unstable. It merges with the trivial solution at $\mu=0$, which is known as the (trans)critical bifurcation point. The solution $|C|^2_+$ is always non-zero, exists for $\mu>-1/4\beta$, and is stable. It merges with $|C|^2_-$ at the turning point $\mu=-1/4\beta$. Thus, in the subcritical regime, $-1/4\beta<\mu<0$, there are two stable homogeneous solutions separated by an unstable one, a typical behavior of a hysteretic system. Equation (17) also allows for bifurcations into different spatial patterns.

For $\beta=1$, the coexistence of the solutions, $|C|=0$ and $|C|^2_+=(1+\sqrt{1+4\mu})/2$, allows for a front solution between these two homogeneous states. At the *Maxwell point*, i.e. for $\mu=\mu_M=-3/16$, the front between the two states is motionless[22]. Here, the potential whose variation gives rise to the right hand side of Eq. (17), has the same value for both states. The front solution at this point is

$$
C^{\mu_M}_{\pm}(\zeta)=\frac{\sqrt{3}}{2}\frac{e^{i\varphi}}{\sqrt{1+e^{\pm\frac{1}{2}\sqrt{3}(\zeta-\zeta_0)}}}, \qquad (18)
$$

where φ is an arbitrary phase and ζ_0 is the front's core position. By moving away from the Maxwell point, the front dynamics is usually characterized by the motion of the center of the front, which is defined as the front position with the largest slope. The front propagates from the global stable (global minimum) to a metastable one (local minimum).[23]

In the general case ($\beta\neq 1$) localized states are possible at the Maxwell point, $\mu=\mu_M$. They are explicitly given by

$$
C_H(\zeta)=\frac{\sqrt{3}}{2}\frac{e^{i\varphi}}{\sqrt{h(\zeta)}} \qquad (19)
$$

with

$$
h(\zeta)=1+e^{\frac{1}{2}\sqrt{3}(\zeta-\zeta_0)}-\frac{1}{4}(\beta-1)e^{-\frac{1}{2}\sqrt{3}(\zeta-\zeta_0)} \qquad (20)
$$

and converge for $\beta\to 1$ to the standard front solution, Eq.(18).

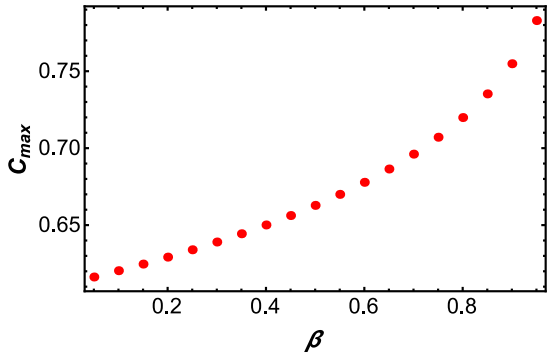

FIG. 5. Maximum amplitude of the localized states, Eq. (19), as a function of β for $\zeta_0 = 0$.

Figure 4 shows the front solution as well as different localized states for different values of β. In the case of $\beta = 1$ only the front solution exists, while the homoclinic orbits are found for $\beta < 1$. As is shown in Fig. 5, the maximum amplitude of the localized states increases for increasing β. We remark that these solutions are unstable away from the Maxwell point.

C. Onset of oscillatory convection

The procedure of deriving the amplitude equation in the stationary case is similar to that of the stationary one, cf. Sec. IV A. The linear solution, $\mathbf{u}_0 = [A_1 \exp(ik_{oc}x) + A_2 \exp(-ik_{oc}x)]\bar{\mathbf{u}}_0(z)\exp(i\omega_{oc}t) + c.c.$ contains two amplitudes, $A_{1,2}$ for the left and right travelling waves.[20] Using $\varepsilon^2 = (Ra - Ra_{oc})/Ra_{oc}$ as expansion parameter the solvability condition in $O(\varepsilon^{7/2})$ renders a set of two coupled complex cubic-quintic Ginzburg-Landau equations,[24,25] describing the slow dynamics of $A_i(X,T)$ in the long wavelength limit

$$\Lambda_0 \frac{\partial A_1}{\partial T} = \Lambda_1 \frac{\partial^2 A_1}{\partial X^2} + \varepsilon^4 \Lambda_2 A_1 + \left(\varepsilon^2 \Lambda_3 |A_1|^2 + \varepsilon^2 \Lambda_4 |A_2|^2 + \Lambda_5 |A_1|^4 + \Lambda_6 |A_2|^4\right) A_1, \quad (21)$$

$$\Lambda_0 \frac{\partial A_2}{\partial T} = \Lambda_1 \frac{\partial^2 A_2}{\partial X^2} + \varepsilon^4 \Lambda_2 A_2 + \left(\varepsilon^2 \Lambda_3 |A_2|^2 + \varepsilon^2 \Lambda_4 |A_1|^2 + \Lambda_5 |A_2|^4 + \Lambda_6 |A_1|^4\right) A_2. \quad (22)$$

The coefficients $\{\Lambda_n\}$ with $n = (0,..,6)$ are complex functions of the parameters and are given in the Appendix.

Figure 6 shows the real and imaginary parts of the quintic saturation coefficient, Λ_5, as a function of the Lewis number $L \in \{0.5, 5\}$ for three different values of the separation ratio $\psi = -0.1, -0.2$, and -0.3 at the porosity number $\chi = 1$. The real part (top) is negative for the material parameters chosen. It decreases with increasing L and decreases with decreasing ψ. To the contrary, the imaginary part (bottom) is positive and increases with increasing L, except for very small L, where it shows a minimum. There is only a very slight dependence on ψ.

Figure 7 shows on the top (bottom) the real (imaginary) part of the quintic coupling coefficient, Λ_6, as a function of L for different values of ψ at $\chi = 1$. Both parts are positive and show a minimum at some smaller value of L, and decrease with increasing ψ.

Finally, we remark that Eqs. (21) and (22) can be used to study secondary instabilities, such as traveling and standing waves, and the Benjamin-Feir instability.[21] These equations can also describe interesting spatiotemporal behavior, like solitons, breathers, localized chaos and more.[26–36]

V. FINAL REMARKS

In this article, we have reported both theoretical and numerical results on convection in binary liquids in a porous medium. We have presented the derivation of the amplitude equations in the subcritical regime result-

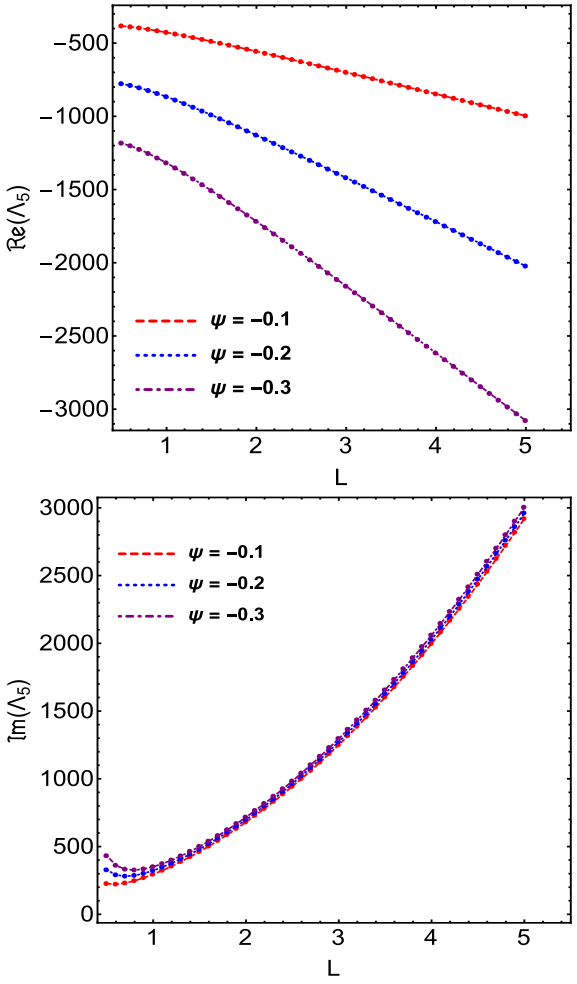

FIG. 6. Real (top) and imaginary (bottom) parts of the quintic coupling coefficient Λ_5 as a function of L for different values of ψ at $\chi = 1$.

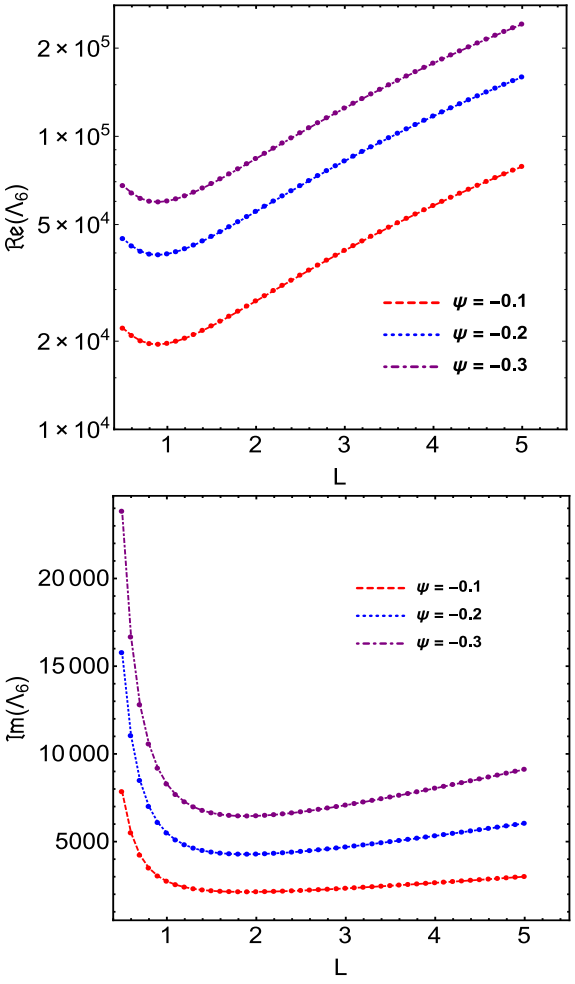

FIG. 7. Real (top) and imaginary (bottom) parts of the quintic saturation coefficient Λ_6 as a function of L for different values of ψ for $\chi = 1$.

ing in a real (complex) cubic-quintic Ginzburg-Landau equation for the stationary (oscillatory) case.

The dependence of the cubic and the quintic coefficients on the material parameters are discussed, and the existence range of the subcritical regime in parameter space is explored for the stationary instability. For a certain ratio between the cubic and quintic coefficient, a front solution is possible that relates two different homogeneous states. An analytical expression is given for that solution at the Maxwell point, where the front is motionless. More generally, within the subcritical regime localized states are found analytically, which are stable at the Maxwell point, but decay away from it.

For the oscillatory convection, we give analytical expressions for the complex coefficients of the amplitude equations in terms of the material parameters and the critical, critical Rayleigh number, critical wavelength, and critical frequency. The critical instability values, however, are known as functions of the material parameters only numerically in the general case. This is used to show the dependence of the real and imaginary part of the quintic coupling coefficient and the quintic saturation coefficient on the material parameters for a small finite porosity number.

The complete study of the space parameter in the subcritical regime for the oscillatory bifurcation is still in progress and will be presented in future works.

ACKNOWLEDGEMENTS

D.L. acknowledges the partial financial support from Basal Program Center for Development of Nanoscience and Nanotechnology (CEDENNA), CONICYT ANILLO ACT 1410 (Chile), startup funding at Yachay Tech University (Ecuador) and GIAN program (India).

Appendix A: Coefficients of the cubic-quintic complex GL equation

The complex coefficients Λ_j with $j = (0,...,6)$ of the cubic-quintic complex GL Eqs. (21) and (22) are split into their real and imaginary parts, $\Lambda_j = \Lambda_{j,R} + i\Lambda_{j,R}$. They are given analytically in this Appendix as functions of L, ψ, and χ with the abbreviations $Q = q_{oc}^2$, $D = \pi^2 + q_{oc}^2$, $\omega = \omega_{oc}$, and $R = Ra_{oc}$, which are:

$$\Lambda_{0,R} = L\chi D^3 + (L+1)D^2 - 3\chi D\omega^2 - (\psi+1)QR \tag{A1}$$

$$\Lambda_{0,I} = 2\omega D\left([L+1]\chi D + 1\right) \tag{A2}$$

$$\begin{aligned}\Lambda_{1,R} = {} & \frac{4\pi^2(L+1)\chi(L^2+\psi[L^2+L+1])D^2}{\psi+1} + LD^2 \\ & -4LD - 12LDQ - R(L\psi+L+\psi)(D+Q) \\ & +4(L+1)\chi Q\omega^2 + 2(L+1)\chi\omega^2 - \omega^2\end{aligned} \tag{A3}$$

$$\begin{aligned}\Lambda_{1,I} = {} & \chi\omega\left(LD^2 - 60QD\right) + 12\chi\omega D\pi^2\left(L^2 + \frac{\psi[L+1]}{\psi+1}\right) \\ & -\chi\omega^3 + \omega D(-\chi L + L + \chi + 1) \\ & -4\omega Q(L+1) - \omega(L+1+[\psi+1]R)\end{aligned} \tag{A4}$$

$$\Lambda_{2,R} = R(\psi L + \psi + L)DQ \tag{A5}$$

$$\Lambda_{2,I} = R(\psi+1)Q\omega \tag{A6}$$

$$\Lambda_{3,R} = \frac{\psi DQR\left([L^3+L]D+1\right)}{8\pi^2L^2} + \frac{(L\psi+\psi)DQR}{8\pi^2} \tag{A7}$$

$$\Lambda_{3,I} = \frac{\psi DQR\left([L^3+L]D+1\right)}{8\pi^2L^2} + \frac{QR\omega}{8\pi^2} \tag{A8}$$

$$\Lambda_{4,R} = \frac{DQ\psi R\left(DL[L^2+1]+1\right)}{8\pi^2L^2} + \frac{L\psi D\left(LD^2+\omega^2\right)}{L^2D^2+\omega^2} + (DQL[\psi+1)]+1)\left(\frac{\pi^2R}{4D^2-\omega^2}+\frac{R}{8\pi^2}\right) + \frac{4\pi^2DR\omega^2\left([L-1]D+Q\right)}{\left(4D^2+\omega^2\right)^2} \tag{A9}$$

$$\Lambda_{4,I} = -\frac{4\pi^2LD^2R\omega}{\left(4D^2+\omega^2\right)^2}\left(\frac{\psi\left(LD^2+\omega^2\right)}{L^2D^2+\omega^2}+(\psi+1)Q\right) + \omega\left([L-1]\delta+Q\right)\left(\frac{\pi^2R}{4D^2-\omega^2}+\frac{R}{8\pi^2}\right) + \frac{\omega\psi QR(\left[L^3+L\right]D+1)}{8\pi^2L^2} \tag{A10}$$

$$\Lambda_{5,R} = \frac{\psi D^2QR\left(L^3D^3\left[L^3+1\right]+\omega^2\left[L\left(D\left[L^3+1\right]+R-\pi\right)-1\right]-L^2D^2\left[\pi L+R+1\right]\right)}{16\pi^2L^3\left(D^2+\omega^2\right)\left(L^2D^2+\omega^2\right)} + \frac{QR\psi}{16\pi^2\left(D^2+\omega^2\right)}\left((L+1)D^2-\frac{\omega^3\left(L^2D^2+[L+1]D+\omega^2\right)}{L^3\left(L^2D^2+\omega^2\right)}\right) \tag{A11}$$

$$\Lambda_{5,I} = \frac{\psi DQR\omega\left(L\left[\omega^2\left(\left[L^3+1\right]D+R-\pi\right)+L^2\left(L^3+1\right)D^3-LD^2\left(\pi L+R+1\right)\right]-\omega^2\right)}{16\pi^2L^3\left(D^2+\omega^2\right)\left(L^2D^2+\omega^2\right)} + \frac{\psi DQR\omega\left(L^2D^2+[L+1]D+\omega^2\right)}{16\pi^2L^3\left(D^2+\omega^2\right)\left(L^2D^2+\omega^2\right)} + \frac{DQR\omega^2}{16\pi^2\left(D^2+\omega^2\right)} \tag{A12}$$

$$\Lambda_{6,R} = \Gamma_1(L\psi+\psi)DQ - \Gamma_2\omega^2 + \Gamma_3 \tag{A13}$$

$$\Lambda_{6,I} = \Gamma_2(L\psi+\psi)DQ + \Gamma_1\omega^2 + \Gamma_4 \tag{A14}$$

where

$$\Gamma_1 = \frac{\pi^2DR\left(32\pi^8L^2+4\pi^4[(L-2)L-2]\omega^2-\omega^4\right)}{4\left(\omega^2+4\pi^4\right)\left(4\pi^4L^2+\omega^2\right)^2\left(D^2+\omega^2\right)} + \frac{DR}{16\pi^2L^2\left(D^2+\omega^2\right)} + \frac{\pi^7\omega\left(4\pi L\left[64\pi^8L^4+32\pi^4L^2\omega^2+\pi^3L+4\omega^4\right]-\omega^2\right)}{4\left(\omega^2+4\pi^4\right)\left(4\pi^4L^2+\omega^2\right)^4} \tag{A15}$$

$$\Gamma_2 = \frac{\pi^9DR^2\omega^2(1-2L\omega^2)\left(4\pi^4L^2-\omega^2\right)+2\pi^4LD^2R^2\omega(\omega^2+8\pi^4)(4\pi^4L^2+\omega^2)^2}{2\left(\omega^2+4\pi^4\right)\left(D^2+\omega^2\right)^2\left(4\pi^4L^2+\omega^2\right)^4} - \frac{\pi^4DR\omega(4\pi^4L^2-\omega^2)}{2\left(4\pi^4L^2+\omega^2\right)^2\left(D^2+\omega^2\right)\left(\omega^2+4\pi^4\right)} \tag{A16}$$

$$\Gamma_3 = -\frac{\Gamma_2(L-1)L\psi DQ\omega}{\pi^4L^2+\omega^2} + \frac{\Gamma_1L\psi Q\left(LD^2+\omega^2\right)}{\pi^4L^2+\omega^2} + \Phi_0L\psi D^2Q - \Phi_1L\psi DQ\omega \tag{A17}$$

$$\Gamma_4 = \frac{\Gamma_1(L-1)L\psi DQ\omega}{\pi^4L^2+\omega^2} + \frac{\Gamma_2L\psi Q\left(LD^2+\omega^2\right)}{\pi^4L^2+\omega^2} - L\Phi_0\psi D^2Q + L\Phi_1\psi D^2Q \tag{A18}$$

with

$$\Phi_0 = \frac{DR}{16\pi^2L^2\left(D^2+\omega^2\right)} + \frac{4\pi^9L^2R\omega^2\left(\omega^2-4\pi^4L\right)}{\left(\omega^2+4\pi^4\right)\left(4\pi^4L^2+\omega^2\right)^2\left(D^2+\omega^2\right)} - \frac{\pi^4R\omega^2\left(L^2D^2+[L+1]D+\omega^2\right)}{\left(4\pi^4L^2+\omega^2\right)\left(D^2+\omega^2\right)\left(L^2D^2+\omega^2\right)} - \frac{2\pi^6L\omega^2\left(4\pi^5L[L+1]DR+\left(\omega^2+4\pi^4\right)\left(D^2+\omega^2\right)\right)}{\left(\omega^2+4\pi^4\right)\left(4\pi^4L^2+\omega^2\right)^2\left(D^2+\omega^2\right)} + \frac{\pi^2R\left(4\pi^4L^2-\omega^2\right)\left(L^2D^3[R+1]+D\omega^2(1-LR)\right)}{4L\left(4\pi^4L^2+\omega^2\right)^2\left(D^2+\omega^2\right)\left(L^2D^2+\omega^2\right)} + \frac{\pi^3R\left(4\pi^4L^2-\omega^2\right)\left(D\left(\omega^2+4\pi^4\right)^2\left(4\pi^4L^2+\omega^2\right)-8\pi^6L(L+1)\omega^2\right)}{4\left(\omega^2+4\pi^4\right)^2\left(4\pi^4L^2+\omega^2\right)^3\left(D^2+\omega^2\right)} + \frac{\pi^6L\left(4\pi^4L^2-\omega^2\right)\left(\pi DR\left(4\pi^4L-\omega^2\right)+\left(\omega^2+4\pi^4\right)\left(D^2+\omega^2\right)\right)}{\left(\omega^2+4\pi^4\right)\left(4\pi^4L^2+\omega^2\right)^3\left(D^2+\omega^2\right)} \tag{A19}$$

$$\text{and} \qquad \Phi_1 = -\frac{8\pi^{11}L^2(L+1)R\omega^3}{\left(\omega^2+4\pi^4\right)^2\left(4\pi^4L^2+\omega^2\right)^2\left(D^2+\omega^2\right)} - \frac{\pi^7 LR\omega\left(4\pi^4L-\omega^2\right)\left(4\pi^4L^2-\omega^2\right)}{\left(\omega^2+4\pi^4\right)\left(4\pi^4L^2+\omega^2\right)^3\left(D^2+\omega^2\right)}$$
$$-\frac{\pi^2R\omega\left(4\pi^4L^2-\omega^2\right)\left(L^2D^2+[L+1]D+\omega^2\right)}{4L\left(4\pi^4L^2+\omega^2\right)^2\left(D^2+\omega^2\right)\left(L^2D^2+\omega^2\right)} - \frac{\pi^4R\omega\left(L^2\delta^6[R+1]+D\omega^2(1-LR)\right)}{\left(4\pi^4L^2+\omega^2\right)\left(D^2+\omega^2\right)\left(L^2D^2+\omega^2\right)}$$
$$-\frac{\pi^4\omega\left(4\pi^4L^2-\omega^2\right)\left(4\pi^4D(\pi L[L+1]R+D)+\left[D^2+4\pi^4\right]\omega^2+\omega^4\right)}{2\left(\omega^2+4\pi^4\right)\left(4\pi^4L^2+\omega^2\right)^3\left(D^2+\omega^2\right)}$$
$$-\frac{4\pi^8L^2\omega\left(4\pi^4D[\pi LR+D]+\omega^2\left[D^2-\pi DR+4\pi^4\right]+\omega^4\right)}{\left(\omega^2+4\pi^4\right)\left(4\pi^4L^2+\omega^2\right)^2\left(D^2+\omega^2\right)} - \frac{\pi^5LDR\omega}{\left(4\pi^4L^2+\omega^2\right)\left(D^2+\omega^2\right)} \tag{A20}$$

Finally, let us remark that the critical values of the oscillatory instability, q_{oc}, ω_{oc}, and Ra_{oc}, (abbreviated here as Q, ω, and R, respectively) are also functions of L, ψ, and χ, but generally only known numerically. In the limit $\chi \ll 1$ they are given by Eqs. (9) - (11), respectively.

REFERENCES

[1] S. Chandrashekar, *Hydrodynamic and Hydromagnetic stability* (Oxford University, New York, 1961).
[2] M. Ilyasov, I. Ostermann, and A. Punzi, *Handbook of Geomathematics* (Springer, Berlin, 2010).
[3] K. Pruess, Geothermics **19**, 3 (1990).
[4] M. J. O'Sullivan, K. Pruess, and M. J. Lippmann, Geothermics **30**, 395 (2001).
[5] D. A. Nield and A. Bejan, *Convection in Porous Media* (Springer, Berlin 2012).
[6] H. Brand and V. Steinberg, Physica A **119**, 327 (1983).
[7] H. Brand and V. Steinberg, Phys. Lett. A **93**, 333 (1983).
[8] V. Steinberg and H. R. Brand, J. Chem. Phys. **78**, 2655 (1983).
[9] V. Steinberg and H. R. Brand, J. Chem. Phys. **80**, 431 (1984).
[10] E. Knobloch, Phys. Rev. A **34**, 1538 (1986).
[11] V. Steinberg and H. R. Brand, Phys. Rev. A **30**, 3366 (1984).
[12] M.-C. Charrier-Mojtabi, B. Elhajjar, and A. Mojtabi, Phys. Fluids **19**, 124104 (2007).
[13] B. Elhajjar, M.-C. Charrier-Mojtabi, and A. Mojtabi, Phys. Rev. E **77**, 026310 (2008).
[14] M. Augustin, R. Umla, B. Huke, and M. Lücke, Phys. Rev. A **82**, 056303 (2010).
[15] R. Umla, M. Augustin, B. Huke, and M. Lücke, Phys. Rev. E **84**, 056326 (2011).
[16] A.C. Newell and J.A. Whitehead, J. Fluid Mech. **38**, 279 (1969).
[17] H.R. Brand, P.S. Lomdahl, and A.C. Newell, Physica D **23**, 345 (1986).
[18] M.C. Cross, and P.C. Hohenberg, Rev Mod. Phys. **65**, 851 (1993).
[19] W. Schoöpf and W. Zimmermann, Physical Review E **47**, 1739 (1992).
[20] S. G. Tagare, M. V. Ramana Murthy and Y. Rameshwar, **50**, 3122 (2007).
[21] H. R. Brand, P. C. Hohenberg, and V. Steinberg, Phys. Rev. A **27**, 591 (1983).
[22] Y. Pomeau, Physica D **23**, 3 (1986).
[23] W. van Saarloos, Physics Reports **386**, 29 (2003).
[24] O. Thual and S. Fauve, J. Phys. France **49**, 1829 (1988).
[25] S. Fauve and O. Thual, Phys. Rev. Lett. **64**, 282 (1990).
[26] H. R. Brand and R. J. Deissler, Phys. Rev. Lett. **63**, 2801 (1989).
[27] H. R. Brand and R. J. Deissler, Physica A **204**, 87 (1994).
[28] R. J. Deissler and H. R. Brand, Phys. Rev. Lett. **72**, 478 (1994).
[29] W. van Saarloos and P. C. Hohenberg, Phys. Rev. Lett. **64**, 749 (1990).
[30] O. Descalzi and H. R. Brand, Phys. Rev. E **81**, 026210 (2010).
[31] O. Descalzi, J. Cisternas, D. Escaff, and H. R. Brand, Phys. Rev. Lett. **102**, 188302 (2009).
[32] M. A. Miranda, J. Burguete, H. Mancini and W. González-Viñas, Phys. Rev. E **87**, 032902 (2013).
[33] M. A. Miranda, D. Laroze and W. González-Viñas, J. Phys.: Condens. Matter **25**, 404208 (2013).
[34] N. Akhmediev, J. M. Soto-Crespo and G. Town, Phys. Rev. E **63**, 056602 (2001).
[35] D. Mihalache, D. Mazilu, F. Lederer, H. Leblond and B. A. Malomed, Phys. Rev. A **81**, 025801 (2010).
[36] A. Ankiewics, N. Akhmediev, *Dissipative Solitons: From Optics to Biology and Medicine*, (Springer, Berlin, 2008).